



Feasibility of late acquisition [⁶⁸Ga]Ga-PSMA-11 PET/CT using a long axial field-of-view PET/CT scanner for the diagnosis of recurrent prostate cancer—first clinical experiences

Ian Alberts¹ · George Prenosil¹ · Clemens Mingels¹ · Karl Peter Bohn¹ · Marco Viscione¹ · Hasan Sari^{1,2} · Axel Rominger¹ · Ali Afshar-Oromieh¹

Received: 26 April 2021 / Accepted: 31 May 2021 / Published online: 21 June 2021
© The Author(s) 2021

Abstract

Purpose While acquisition of images in [⁶⁸Ga]Ga-PSMA-11 following longer uptake times can improve lesion uptake and contrast, resultant imaging quality and count statistics are limited by the isotope's half-life (68 min). Here, we present a series of cases demonstrating that when performed using a long axial field-of-view (LAFOV) PET/CT system, late imaging is feasible and can even provide improved image quality compared to regular acquisitions.

Methods In this retrospective case series, we report our initial experiences with 10 patients who underwent standard imaging at 1 h p.i. following administration of 192 ± 36 MBq [⁶⁸Ga]Ga-PSMA-11 with additional late imaging performed at 4 h p.i. Images were acquired in a single bed position for 6 min at 1 h p.i. and 16 min p.i. at 4 h p.i. using a LAFOV scanner (106 cm axial FOV). Two experienced nuclear medicine physicians reviewed all scans in consensus and evaluated overall image quality (5-point Likert scale), lesion uptake in terms of standardised uptake values (SUV), tumour to background ratio (TBR) and target-lesion signal to background noise (SNR).

Results Subjective image quality as rated on a 5-point Likert scale was only modestly lower for late acquisitions (4.2/5 at 4 h p.i.; 5/5 1 h p.i.), TBR was significantly improved (4 h: 3.41 vs 1 h: 1.93, $p < 0.001$) and SNR was improved with borderline significance (4 h: 33.02 vs 1 h: 24.80, $p = 0.062$) at later imaging. Images were obtained with total acquisition times comparable to routine examinations on standard axial FOV scanners.

Conclusion Late acquisition in tandem with a LAFOV PET/CT resulted in improvements in TBR and SNR and was associated with only modest impairment in subjective visual imaging quality. These data show that later acquisition times for [⁶⁸Ga]Ga-PSMA-11 may be preferable when performed on LAFOV systems.

Keywords Total body · Ultra-long FOV PET · Whole body · PET/CT · Positron-emission tomography · Digital PET

Introduction

Recently introduced long axial field-of-view (LAFOV) PET/CT scanners offer significant improvements over previous standard axial FOV (SAFOV) systems [1, 2], with substantially improved sensitivity and count densities [3]. Most recently, the first Siemens Biograph Vision Quadra system (Siemens Healthineers, Knoxville, TN, USA) with an axial FOV of 106 cm was installed at the Department for Nuclear Medicine, University Hospital Bern, in Switzerland. The performance characteristics of this scanner have been investigated previously in phantom studies [4, 5] and in a clinical setting [6].

PET/CT with PSMA radioligands is the modality of choice for the staging of biochemically recurrent prostate

This article is part of the Topical Collection on Oncology—Genitourinary

✉ Ian Alberts
ian.alberts@insel.ch

¹ Department of Nuclear Medicine, Inselspital, Bern University Hospital, University of Bern, Freiburgstr. 18, 3010 Bern, Switzerland

² Advanced Clinical Imaging Technology, Siemens Healthcare AG, Lausanne, Switzerland

cancer (PC). Typically, when performed with [^{68}Ga]Ga-PSMA-11, imaging is routinely performed at 1 h post injection of radiotracer (p.i.) [7–9]. However, this choice of imaging time is drawn from the first clinical description of [^{68}Ga]Ga-PSMA-11, and is not based on a systematic evaluation of the optimal imaging time [7, 10]. Acquisition of images at later time points is associated with improved tumour to background (TBR) and lesion detectability [11–15] and is mentioned in current guidelines [9]. Despite these benefits to later acquisition, limiting factors are encountered: e.g. the short half-life of the radiopharmaceutical (68 min) results in decay at later imaging, and additional scanning can be difficult to integrate into a busy clinical service. This is particularly the case where, as a result of radioisotope decay, longer acquisition times are required to achieve adequate count statistics which can reduce the scanner's availability for other patients [9]. Pioneering publications with LAFOV scanners report increased dynamic range for LAFOV systems, meaning that radiopharmaceuticals can be followed usefully over more half-lives as a result of the scanner's higher sensitivity [1]. The aim of this short communication is to report our initial experiences with a LAFOV scanner in late imaging with [^{68}Ga]Ga-PSMA-11, to demonstrate that later acquisition of imaging is feasible and that even improved image quality can be obtained at late imaging when compared to regular acquisitions.

Materials and methods

Study design

This retrospective case series presents 10 cases who underwent “standard” clinical [^{68}Ga]Ga-PSMA-11 PET/CT on our LAFOV system for biochemically recurrent PC at 1 h p.i. and where additional “late” imaging was performed as per institutional standard. Previously, such additional scans were performed at 2.5 h p.i. using a SAFOV-PET [13]. Cognisant of the higher sensitivity of the LAFOV system, additional late imaging for these patients was performed at 4 h p.i.

Imaging procedures

All scans were performed using the Siemens Biograph Vision Quadra system (axial FOV = 106 cm). Reconstruction parameters were as previously described [13]. Patients underwent a single scan from head to mid thighs in a single bed position (b.p.) with acquisition times of 6 min at 1 h p.i. and 16 min at 4 h p.i. (including an additional low dose CT for attenuation correction) following a single bolus administration of the radiopharmaceutical (192 ± 36 MBq) which was prepared as previously published [16]. Thirty minutes

prior to the late (4 h) scans, 20 mg of intravenous Furosemide was applied following oral hydration in compliance with local protocol [13].

Image analysis

All scans were analysed in a consensus read by two experienced nuclear medicine physicians (first and last author). Scans were analysed first with respect to target lesions according to published interpretation criteria [17]. PET images were displayed in the PET-rainbow colour look-up table using appropriate software (Syngo.Via, Siemens Healthineers) as previously described [18]. Both readers were blinded to both patient demographics and image acquisition details. To minimise recall bias, images were reviewed in randomised order. Images were rated by both readers according to subjective image quality rated on a 5-point Likert scale: (1) very poor; (2) poor; (3) acceptable; (4) very good; (5) excellent. Lesion uptake was measured in terms of SUV_{peak} [19], which has been shown to be a more reliable parameter irrespective of acquisition time than SUV_{max} [20]. The background was defined as the SUV_{mean} of a background volume of interest (VOI) placed in a reference region of healthy liver tissue, where SUV_{mean} was shown to be the most reliable parameter for liver [11, 19]. TBR was defined as lesion SUV_{peak} divided by background SUV_{mean} . SNR was defined as the reciprocal coefficient of variation $\text{SNR} = \mu/\sigma$, where μ = target lesion SUV_{peak} and σ = standard deviation of the liver-background VOI [21]. The data in this case series were analysed descriptively using mean, median and statistical significance testing by means of the paired Student's *t*-test.

Results

Patient characteristics are shown in Table 1. All patients have PSMA-avid prostate cancer lesions, with a total of 20 pathological lesions detected and analysed. As anticipated, subjective image quality (as rated on a Likert scale) was judged to be highest for the acquisitions at 1 h p.i. (mean 5/5), with only modest reduction in visual quality observed at 4 h p.i. (mean 4.2/5, range 4–5) as rated on a 5-point Likert scale.

Later acquisition was associated with higher lesion SUV_{peak} (mean 13.43 vs. 10.07, $p=0.05$; median 8.46 vs. 6.51). Mean TBR was higher at 4 h compared to 1 h (3.41 vs 1.93, $p<0.001$; median 1.55 vs. 1.48); data are shown in Fig. 1. SNR was improved at late acquisition (4 h p.i. 33.02 vs. 1 h p.i. 24.80, $p=0.062$; median 15.1 vs 14.2), with borderline significance owing to the limited data in this case series. Data are shown in Fig. 2. Example patient

Table 1 Patient characteristics: RPE radical prostatectomy, RT radiotherapy, ADT androgen deprivation therapy, None no further treatment, Scan (p.i.) scan time post injection of radiotracer hh:mm. Scan findings: LR local recurrence, LN lymph node, X no PSMA-avid lesions suspicious for PC, pulm pulmonary metastasis

Patient	Age (years)	Body weight (kg)	Applied activity (MBq)	PSA (ng/ml)	Gleason score	Initial therapy	Further therapy	Scan 1 (p.i.)	Scan 2 (p.i.)	Scan findings
1	78	60	217	1.5	9	RPE	ADT	01:05	03:55	LR
2	74	85	210	2.11	8	RPE	RT	01:10	04:08	LR, pelvic LN
3	67	62	146	2.2	7	RPE	RT+ADT	01:03	04:13	LR
4	78	102	211	2.15	7	RT	ADT	01:24	04:25	LR, bone
5	60	85	161	4.52	7	RPE+RT	ADT	01:04	04:02	bone
6	63	60	180	0.44	7	RPE	None	01:01	04:11	LR, pelvic LN
7	75	75	185	5.2	7	RPE	None	01:16	04:05	LR
8	69	108	201	1	7	RPE	None	00:58	04:03	X
9	81	75	210	12.2	7	RT	None	01:13	04:25	Pelvic LN, abdominal LN, thoracic LN, pulm
10	67	80	197	1.25	7	RPE	None	00:57	04:00	LR

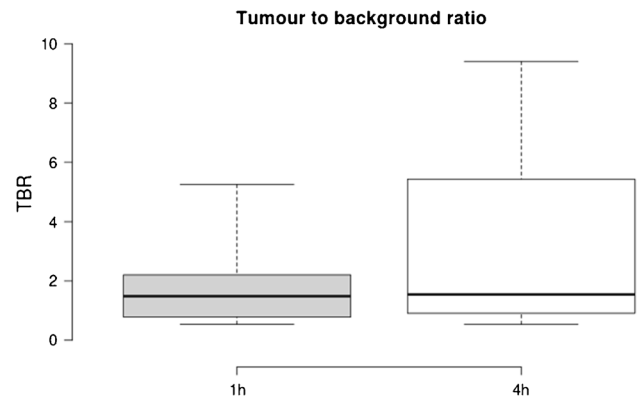


Fig. 1 Shown are boxplots depicting tumour to background (TBR) ratio at 1 h (standard) acquisition, 4 h (late). Improved TBR is seen at 4 h p.i., and no significant reduction ($p=0.5$) is seen with the patients undergoing a low dose protocol compared to standard acquisition. For all boxplots: the median is shown by the central line in bold, the 25th and 75th percentiles are shown by the box limits and whiskers extend to the minima and maxima

images are shown in Fig. 3 and Fig. 4 and additional images in Supplementary Fig. 1 and 2.

Discussion

This case series indicates that late imaging is feasible with [^{68}Ga]Ga-PSMA-11 without relevant loss of image quality, where the sensitivity gains in a LAFOV PET/CT system result in greater dynamic range, i.e. the greater sensitivity of the scanner allows radiotracers to be followed over more half-lives [1].

The pharmacokinetic behaviour of [^{68}Ga]Ga-PSMA-11 is well known, and the majority of tumour lesions show increasing radiotracer uptake over time [7]. It is therefore beneficial to observe the radiotracer over several half-lives,

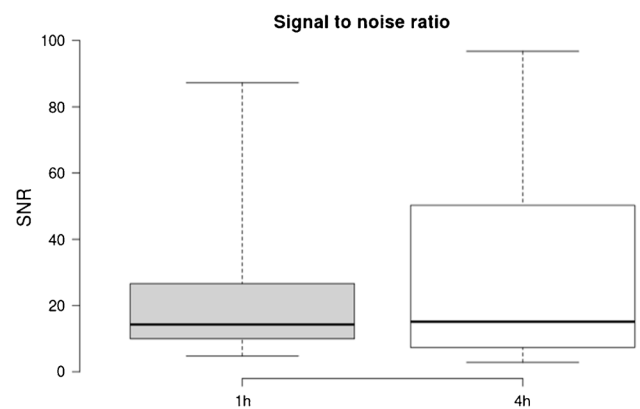


Fig. 2 Signal to noise (SNR) ratio, defined as the reciprocal coefficient of variation for 1 h and 4 h acquisitions. Improved SNR is seen at later imaging

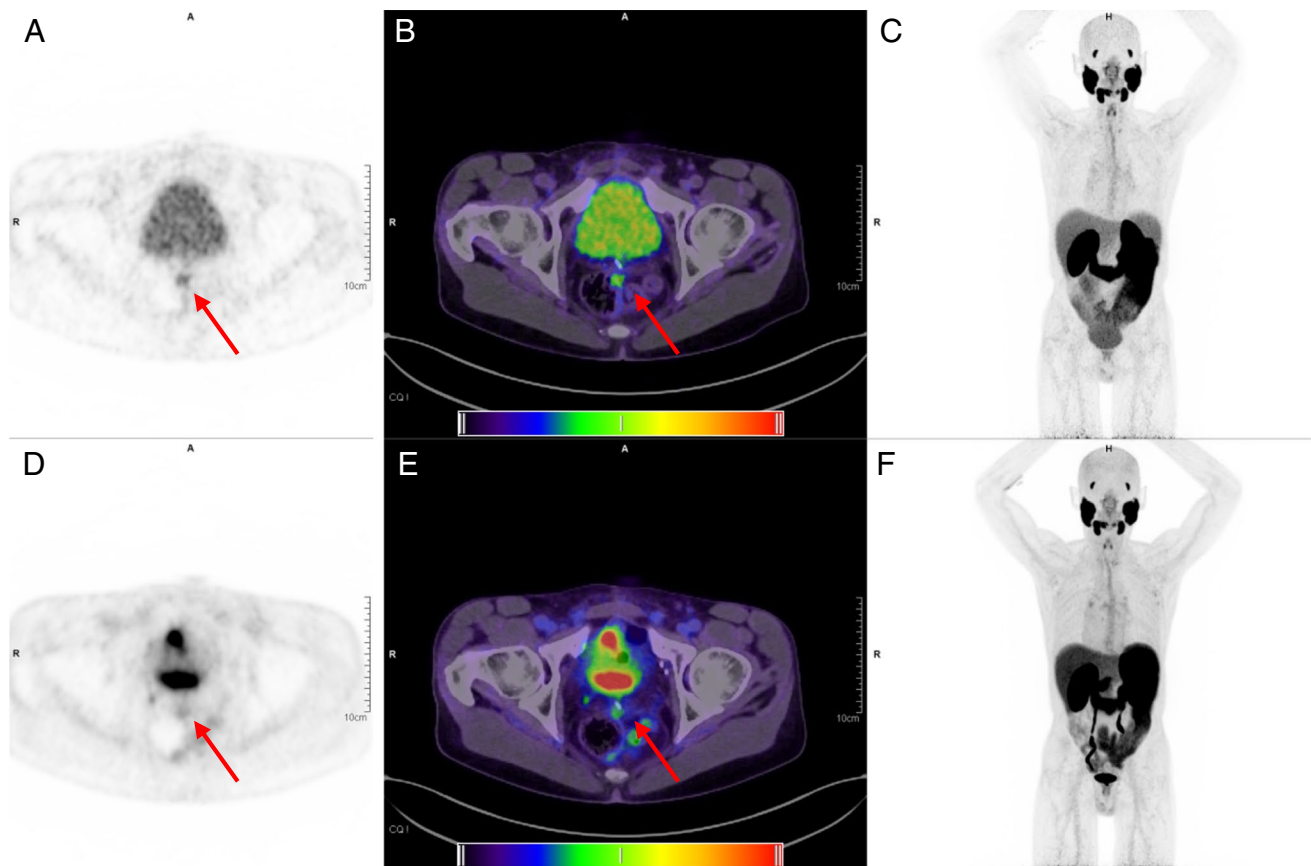


Fig. 3 Illustrative images for an example patient (#3). Shown are images acquired at 4 h p.i. with a 16 min total acquisition time (top row, tiles a–c) and 1 h p.i. images with 6 min total acquisition time (bottom row, tiles d–f). Visual inspection of the two maximal intensity projections (c and f) demonstrates that only a modest reduction

in image quality is seen at late imaging. The locally recurrent lesion (shown by red arrows) at the left mesorectal fascia is faintly visible at 1 h (PET d and fusion PET and CT, e) but more clearly discerned at 4 h (PET a and fusion PET and CT, b). For reference, the PET window was set to 0 and 6 SUV to best display the lesion

which can improve lesion visibility, background tissue clearance and TBR [10–14, 16, 22]. However, dual time point or later imaging is not universally accepted; additional or discretionary imaging can be challenging to integrate into the clinical routines of a busy nuclear medicine department and may require long acquisition times reducing scanner availability. With a mean applied activity for the patients in this report of 192 MBq, after 4 h, less than 17 MBq of the originally applied activity would be available following decay, and in reality even less would be available when considering the biological half-life [7]. With such low amounts of radiopharmaceutical activity remaining, the resultant imaging quality using previous-generation scanners was clinically unacceptable [23]. A standard acquisition using a SAFOV scanner recommended by the guidelines is 2 min/bp, which for a previous generation scanner in continuous bed motion could take up to 16 min (2 min/bp equivalent to 1.1 mm/s table speed [24]). By contrast, the LAFOV scanner is able to capture a 106 cm FOV in a single acquisition, enabling improved acquisition times: for example, a 16 min/bp

acquisition, as we performed at 4 h, would be impracticably long when using a SAFOV system. Whereas later acquisition of images can be to the detriment of image quality using SAFOV systems, this is not the case for LAFOV systems. Moreover, these cases demonstrate the ability to achieve a high-quality image after nearly four half-lives had elapsed, i.e. where >90% of the applied radiopharmaceutical has undergone decay. Although not the aim of this present study, this implies that as alternative to late acquisition, low dose protocols are feasible in LAFOV, for which further dedicated studies are required. Such low-dose protocols are of clinical interest since they might be a method to ameliorate supply bottlenecks for ^{68}Ga [25].

Despite nearly a decade of routine use, the optimal imaging protocol for ^{68}Ga]Ga-PSMA-11 PET/CT remains elusive. Given the improvement in lesion contrast (TBR) and SNR, rather than acquiring images at 1 h p.i., delayed acquisition might be preferable with new-generation LAFOV scanners. We note that later acquisition is recommended for other ^{18}F -labelled PSMA-radiotracers,

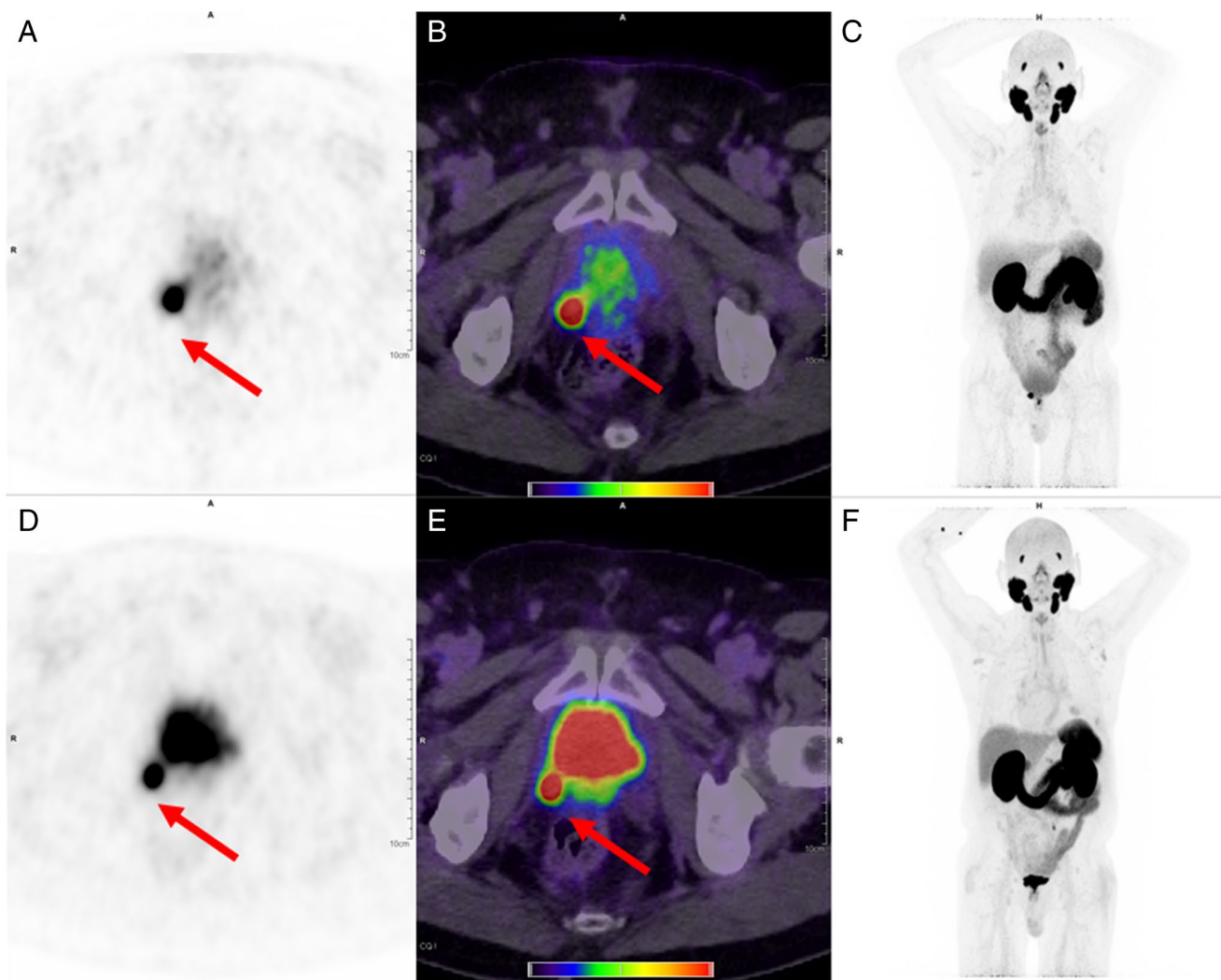


Fig. 4 Illustrative images (patient #8). Shown are the 4 h images (top row) and 1 h images (bottom row). A locally recurrent lesion at the bladder wall (red arrow) is discernible in both the PET (tiles **a** and **d**) and the fusion PET and CT (tiles **b** and **e**), with barely perceptible

visual difference in image quality between the two acquisitions. The combination of diuresis and later acquisition (at 4 h p.i.) results in better lesion demarcation from the bladder (MIP tiles **c** and **f**). Images are shown with PET window 0 to 10 SUV

such as [^{18}F]PSMA-1007 where 2 h p.i. is favoured [26] and where 2 h imaging may be valuable for [^{18}F]DCFPyl [27].

Our short report is limited by the small patient numbers and represents our first experiences in this regard with this new scanner. Although readers were blinded to clinical details and scans were read in randomised order, recall bias cannot be excluded, although this case series does not seek to present a systematic evaluation but rather to demonstrate the feasibility of later image acquisition and imaging quality achievable on a state-of-the-art LAFOV system as a report of first clinical experiences with the first scanner of this type. Although further systematic analyses are required to confirm our findings, we hypothesise that when using LAFOV systems, later acquisitions could be favoured in certain

conditions. Future studies should evaluate other imaging time points, such as 2 h or 3 h p.i.

These initial data demonstrate that, when using a LAFOV scanner, not only are late acquisitions feasible with total acquisition times not exceeding those of a routine scan, but that improvements in terms of TBR and SNR are possible.

Conclusion

In this case series, late acquisition in tandem with a LAFOV PET/CT did not result in reduced imaging quality, however improved TBR and SNR at late imaging. High-quality imaging at a time point when nearly four half-lives for the radiotracer had elapsed was possible within clinically acceptable

total acquisition times. These data show that later acquisition times for [⁶⁸Ga]Ga-PSMA-11 may be preferable when performed on LAFOV systems.

Supplementary Information The online version contains supplementary material available at <https://doi.org/10.1007/s00259-021-05438-5>.

Funding Open Access funding provided by Universität Bern.

Declarations

Ethics approval and consent to participate The cantonal ethics committee provided a waiver for retrospective analysis of this cohort (Req-2021–00141). All patients provided written informed consent for inclusion in this study. The study was performed in accordance with the declaration of Helsinki and relevant national legislation.

Conflict of interest HS is a full-time employee of Siemens Healthcare AG, Switzerland.

AR has received research support and speaker honoraria from Siemens. All other authors have no conflicts of interest to report.

Open Access This article is licensed under a Creative Commons Attribution 4.0 International License, which permits use, sharing, adaptation, distribution and reproduction in any medium or format, as long as you give appropriate credit to the original author(s) and the source, provide a link to the Creative Commons licence, and indicate if changes were made. The images or other third party material in this article are included in the article's Creative Commons licence, unless indicated otherwise in a credit line to the material. If material is not included in the article's Creative Commons licence and your intended use is not permitted by statutory regulation or exceeds the permitted use, you will need to obtain permission directly from the copyright holder. To view a copy of this licence, visit <http://creativecommons.org/licenses/by/4.0/>.

References

- Cherry SR, Jones T, Karp JS, Qi J, Moses WW, Badawi RD. Total-body PET: maximizing sensitivity to create new opportunities for clinical research and patient care. *J Nucl Med Off Publ Soc Nucl Med*. 2018;59:3–12. <https://doi.org/10.2967/jnumed.116.184028>.
- Badawi RD, Shi H, Hu P, Chen S, Xu T, Price PM, et al. First human imaging studies with the EXPLORER total-body PET scanner. *J Nucl Med Off Publ Soc Nucl Med*. 2019;60:299–303. <https://doi.org/10.2967/jnumed.119.226498>.
- Spencer BA, Berg E, Schmall JP, Omidvari N, Leung EK, Abdelhafez YG, et al. Performance evaluation of the uEXPLORER total-body PET/CT scanner based on NEMA NU 2–2018 with additional tests to characterize long axial field-of-view PET scanners. *J Nucl Med*. 2020;jnumed.120.250597. <https://doi.org/10.2967/jnumed.120.250597>.
- Siegel S, Aykac M, Bal H, Bendriem B, Bharkhada D, Cabello J, et al. Preliminary performance of a prototype, one-meter long PET tomograph. *IEEE NSS-MIC*. Boston, MA: IEEE; 2020.
- Prenosil GA, Sari H, Fürstner M, et al. Performance characteristics of the biograph vision quadra PET/CT system with long axial field of view using the NEMA NU 2-2018 Standard. *J Nucl Med*; 2021. (in press).
- Alberts I, Hünermund J-N, Prenosil G, Mingels C, Bohn KP, Viscione M, et al. Clinical performance of long axial field of view PET/CT: a head-to-head intra-individual comparison of the Biograph Vision Quadra with the Biograph Vision PET/CT. *European J Nucl Med Mol Imaging*. 2021. <https://doi.org/10.1007/s00259-021-05282-7>.
- Afshar-Oromieh A, Malcher A, Eder M, Eisenhut M, Linhart HG, Hadaschik BA, et al. PET imaging with a [68Ga]gallium-labelled PSMA ligand for the diagnosis of prostate cancer: biodistribution in humans and first evaluation of tumour lesions. *Eur J Nucl Med Mol Imaging*. 2013;40:486–95. <https://doi.org/10.1007/s00259-012-2298-2>.
- Afshar-Oromieh A, da Cunha ML, Wagner J, Haberkorn U, Debus N, Weber W, et al. Performance of [68Ga]Ga-PSMA-11 PET/CT in patients with recurrent prostate cancer after prostatectomy—a multi-centre evaluation of 2533 patients. *Eur J Nucl Med Mol Imaging*. 2021. <https://doi.org/10.1007/s00259-021-05189-3>.
- Fendler WP, Eiber M, Beheshti M, Bomanji J, Ceci F, Cho S, et al. (68)Ga-PSMA PET/CT: Joint EANM and SNMMI procedure guideline for prostate cancer imaging: version 1.0. *Eur J Nucl Med Mol Imaging*. 2017;44:1014–24. <https://doi.org/10.1007/s00259-017-3670-z>.
- Afshar-Oromieh A, Hetzheim H, Kubler W, Kratochwil C, Giesel FL, Hope TA, et al. Radiation dosimetry of (68)Ga-PSMA-11 (HBED-CC) and preliminary evaluation of optimal imaging timing. *Eur J Nucl Med Mol Imaging*. 2016;43:1611–20. <https://doi.org/10.1007/s00259-016-3419-0>.
- Alberts I, Sachpekidis C, Gourni E, Boxler S, Gross T, Thalmann G, et al. Dynamic patterns of [68Ga]Ga-PSMA-11 uptake in recurrent prostate cancer lesions. *Eur J Nucl Med Mol Imaging*. 2020;47:160–7. <https://doi.org/10.1007/s00259-019-04545-8>.
- Schmuck S, Mamach M, Wilke F, von Klot CA, Henkenberens C, Thackeray JT, et al. Multiple time-point 68Ga-PSMA I&T PET/CT for characterization of primary prostate cancer: value of early dynamic and delayed imaging. *Clin Nucl Med*. 2017;42.
- Alberts I, Huenermund JN, Sachpekidis C, Zacho HD, Mingels C, Dijkstra L, et al. Combination of forced diuresis with additional late imaging in 68Ga-PSMA-11 PET/CT—effects on lesion visibility and radiotracer uptake. *J Nucl Med*. 2021;jnumed.120.257741. <https://doi.org/10.2967/jnumed.120.257741>.
- Hoffmann MA, Buchholz H-G, Wieler HJ, Rosar F, Miederer M, Fischer N, et al. Dual-time point [68Ga]Ga-PSMA-11 PET/CT hybrid imaging for staging and restaging of prostate cancer. *Cancers*. 2020;12. doi:<https://doi.org/10.3390/cancers12102788>.
- Afshar-Oromieh A, Sattler LP, Mier W, Hadaschik BA, Debus J, Holland-Letz T, et al. The clinical impact of additional late PET/CT imaging with 68Ga-PSMA-11 (HBED-CC) in the diagnosis of prostate cancer. *J Nucl Med*. 2017;58:750. <https://doi.org/10.2967/jnumed.116.183483>.
- Alberts I, Sachpekidis C, Dijkstra L, Prenosil G, Gourni E, Boxler S, et al. The role of additional late PSMA-ligand PET/CT in the differentiation between lymph node metastases and ganglia. *Eur J Nucl Med Mol Imaging*. 2020;47:642–51. <https://doi.org/10.1007/s00259-019-04552-9>.
- Rowe SP, Pienta KJ, Pomper MG, Gorin MA. PSMA-RADS Version 1.0: a step towards standardizing the interpretation and reporting of PSMA-targeted PET imaging studies. *Eur Urol*. 2018;73:485–7. <https://doi.org/10.1016/j.eururo.2017.10.027>.
- Mingels C, Sachpekidis C, Bohn KP, Hünermund J-N, Schepers R, Fech V, et al. The influence of colour scale in lesion detection and patient-based sensitivity in [68Ga]Ga-PSMA-PET/CT. *Nuclear Medicine Communications*. 2021; Publish Ahead of Print.
- Sher A, Lacoëuille F, Fosse P, Vervueren L, Cahouet-Vannier A, Dabli D, et al. For avid glucose tumors, the SUV peak is the most reliable parameter for [(18)F]FDG-PET/CT quantification, regardless of acquisition time. *EJNMMI Res*. 2016;6:21. <https://doi.org/10.1186/s13550-016-0177-8>.

20. Prenosil GA, Weitzel T, Furstner M, Hentschel M, Krause T, Cumming P, et al. Towards guidelines to harmonize textural features in PET: Haralick textural features vary with image noise, but exposure-invariant domains enable comparable PET radiomics. *PLoS ONE*. 2020;15. <https://doi.org/10.1371/journal.pone.0229560>.
21. Yan J, Schaefferkoetter J, Conti M, Townsend D. A method to assess image quality for low-dose PET: analysis of SNR, CNR, bias and image noise. *Cancer Imaging*. 2016;16:26. <https://doi.org/10.1186/s40644-016-0086-0>.
22. Haupt F, Dijkstra L, Alberts I, Sachpekidis C, Fecht V, Boxler S, et al. 68Ga-PSMA-11 PET/CT in patients with recurrent prostate cancer—a modified protocol compared with the common protocol. *Eur J Nucl Med Mol Imaging*. 2020;47:624–31. <https://doi.org/10.1007/s00259-019-04548-5>.
23. Rauscher I, Fendler WP, Hope T, Quon A, Nekolla SG, Calais J, et al. Can the injected dose be reduced in 68Ga-PSMA-11 PET/CT maintaining high image quality for lesion detection? *J Nucl Med*. 2019. <https://www.siemens-healthineers.com/molecular-imaging/optics-and-upgrades/software-applications/flowmotion-technology>.
25. Mueller D, Fuchs A, Leshch Y, Proehl M. The shortage of approved 68Ga generators-incoming material inspection and GMP compliant use of non-approved generators. *J Nucl Med*. 2019;60:1059-.
26. Giesel FL, Hadaschik B, Cardinale J, Radtke J, Vinsensia M, Lehnert W, et al. F-18 labelled PSMA-1007: biodistribution, radiation dosimetry and histopathological validation of tumor lesions in prostate cancer patients. *Eur J Nucl Med Mol Imaging*. 2017;44:678–88. <https://doi.org/10.1007/s00259-016-3573-4>.
27. Szabo Z, Mena E, Rowe SP, Plyku D, Nidal R, Eisenberger MA, et al. Initial evaluation of [18F]DCFPyL for prostate-specific membrane antigen (PSMA)-targeted PET imaging of prostate cancer. *Mol Imaging Biol*. 2015;17:565–74. <https://doi.org/10.1007/s11307-015-0850-8>.

Publisher's Note Springer Nature remains neutral with regard to jurisdictional claims in published maps and institutional affiliations.